



Exploring Enhanced Forced Convection With Pcm: A Numerical Study On Heat Transfer Improvement In Literature

S BALA MOHAN¹ & DR B OMPRAKASH²

¹Research Scholar, Department of Mechanical Engineering, JNTUA College of Engineering and Technology, Anantapuramu, Andhra Pradesh.

²Assistant Professor, Department of Mechanical Engineering, JNTUA College of Engineering and Technology, Anantapuramu, Andhra Pradesh.

ABSTRACT:

This review aims to examine the mathematical assessment of improving heat transmission in forced convection scenarios by employing Phase Change Materials (PCMs). The analysis commences with an examination of the fundamental principles underlying forced convection, followed by a detailed description of the mechanism responsible for forced convection is provided. The subsequent emphasis is directed towards Phase Change Materials (PCMs), encompassing many classifications and their utilization in heat transfer, encompassing domains such as solar energy, building applications, and vehicle applications. This paper presents mathematical models that investigate phase change materials (PCMs) flow and heat transfer. The models take into account fixed grids, adaptive meshes, as well as first law and second law models inside computational domains. This review gives a thorough assessment among the numerical methodologies used to simulate phase change material (PCM) energy transport. Front-tracking techniques and also fixed grid processes namely a substance's apparent thermal capacity, and source-based methods approach, are comprehensively investigated. Furthermore, this study delves into the exploration of heat transfer augmentation technologies, such as the utilization materials with low density, porous materials, and also metal matrices. The inquiry culminates by providing a concise overview of the principal discoveries and knowledge acquired through an extensive examination of numerical methodologies and technologies utilized to improve heat transfer in forced convection applications involving Phase Change Materials.

KEYWORDS: phase change material (PCM), forced convection, heat transfer, numerical techniques, enthalpy method.

Introduction

The use of numerical studies has played a critical role in improving understanding of heat transfer processes, especially in the context of convection-forced applications utilizing PCMs are phase change materials. The capacity to store as well as release thermal energy during phase transitions is unique to phase change materials (PCMs). This characteristic presents a distinct chance to augment the efficiency of heat transmission in diverse systems. To model the complicated dynamics between fluid flow and also phase change material (PCM) in forced convection situation, 'finite element analysis (FEA)' and 'computational fluid dynamics (CFD)' are often utilised computer methodologies. The current simulations look at the implications of incorporating phase change materials (PCMs) on increasing heat transfer. Several characteristics are included in the numerical models, including the exact phase change material (PCM) utilized, its unique melting including freezing properties, and the spatial arrangement within the system. This allows a comprehensive examination of how forced convection systems including phase change materials (PCMs) might reduce temperature variations and enhance thermal efficiency.



Numerical investigations additionally priorities the optimization of parameters such as flow rates, input temperatures, and in order to identify the circumstances that result in phase change material fractions of volume (PCM), most substantial enhancements in heat transfer. In addition, scholars examine the transitory dynamics of the system in the context of phase transitions in order to get insights on the temporal dimensions of augmenting heat transport. The knowledge acquired from these quantitative experiments provides a foundation for the advancement of thermal power storage technologies that exhibit enhanced efficacy and improved environmental sustainability. Applications include a diverse array of fields, including HVAC Thermal (heating, ventilation, and air conditioning) systems power plants, including electronics cooling. Researchers provide a valuable contribution to the advancement of energy efficiency and sustainability in many technological applications by incorporating phase change materials (PCMs) into forced convection scenarios and using numerical simulations.

Fundamentals of Forced Convection

Convection is a method of heat transmission that occurs inside a fluid when there is concurrent movement of the fluid as a whole. The classification of convection is based on the initiation of fluid motion, distinguishing between natural (or free) convection as well as forced convection are two types of convection. Natural convection is the phenomena that occurs when natural processes such as the buoyancy effect produce fluid motion. This phenomenon is characterized by the upward migrating of warmer fluid paired with the downward tendency of colder fluid. The fluid in convection that is forced is pushed to cross a surface and conduit by external forces that include a pump or fan [1].

Forced Convection Mechanism

Convection heat transmission is intricate due to the simultaneous presence of fluid motion and heat conduction. The smooth movement improves the transfer of heat (with a higher velocity cause the rate of heat transmission to increase).

$$q_{conv} = h(T_s - T_\infty)(W / m^2)$$

(1)

$$\dot{Q}_{conv} = hA(T_s - T_\infty)(W)$$

(2)

Fluid properties, Surface roughness, as well as flow type (laminar or turbulent), all have a substantial influence on convective heat exchanges h.

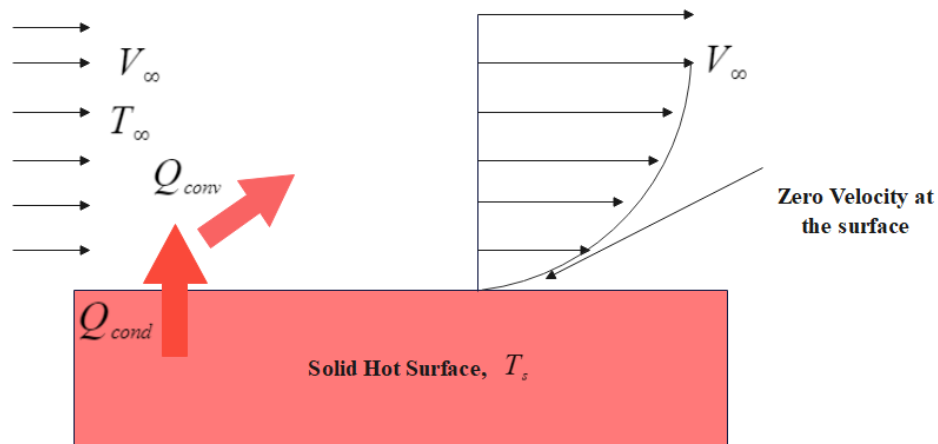


Figure 1: Forced convection

Assuming the fluid's velocity is zero near the wall is the basis of the no-slip condition. As a result, the fluid stays put and heat is transferred only via conduction from the solid surface to the adjacent layer of fluid. Hence,

$$\dot{q}_{conv} = \dot{q}_{cond} = -k_{fluid} \left. \frac{\partial T}{\partial y} \right|_{y=0} \} \rightarrow h = \frac{-k_{fluid} \left. \frac{\partial T}{\partial y} \right|_{y=0}}{T_s - T_\infty} \text{ (W / m}^2\text{)}$$

$$\dot{q}_{conv} = h(T_s - T_\infty)$$

(3)

Phase Change Materials (PCMs)

When PCMs go through physical state transitions, like going from a solid to a liquid or a liquid to a solid, they absorb or emit a lot of "latent" heat (Fig 2). Regardless of whether the substance is being heated or cooled, the phase shift happens when its temperature exceeds the threshold temperature for phase transition. Whether the PCM is absorbing or releasing latent heat, its temperature stays the same. Several final goods can benefit from the PCM's ability to regulate the efficient absorption and release of large amounts of heat. One interesting property of the PCM is its ability to store latent heat. PCMs are well-known for their exceptional heat storing capabilities [2].

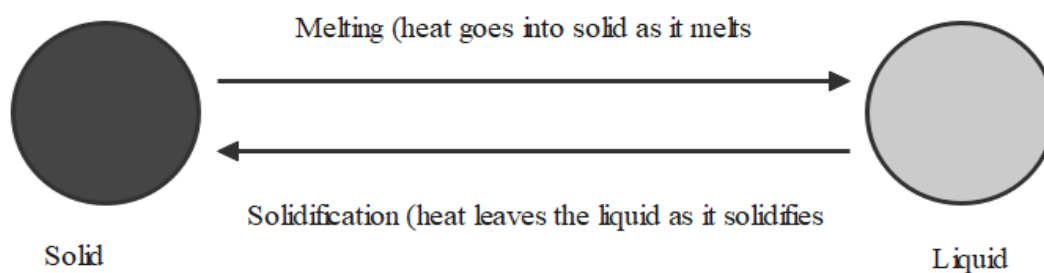


Figure 2: Diagrammatic illustration of the phase-change procedure

[3] Presented a summary of the fundamental principles underlying phase change materials (PCMs) and examine various research approaches employed to improve energy storage capacity and optimise the efficiency of PCMs. When optimising, it is crucial to consider two criteria when selecting a phase change material (PCM): "latent heat and phase transition temperature". Due to its unique geometric features, a spherical tank containing a phase change material (PCM) experiences almost no heat loss. Nevertheless, considering the intricate spatial demands of the tank and the manufacturing process, employing a cylindrical water tank that incorporates Phase Change Material (PCM) emerges as a more rational and viable solution.

Types of PCMs

Figure 3 shows one way to categorize PCMs, although in general, there are two main categories: Paraffin wax (an organic PCM) and salt hydrates (an inorganic PCM) are two examples of polar comonomers [4]. Inorganic phase change materials (PCMs) were employed in the earliest attempts to build latent TES materials. Glauber's salt (sodium sulphate decahydrate) is one example of a salt hydrate that was investigated intensively in the early days of PCM research [5]. Table 1 displays the phase change properties of inorganic PCMs [6], while table 2 displays a promising selection of organic PCMs.

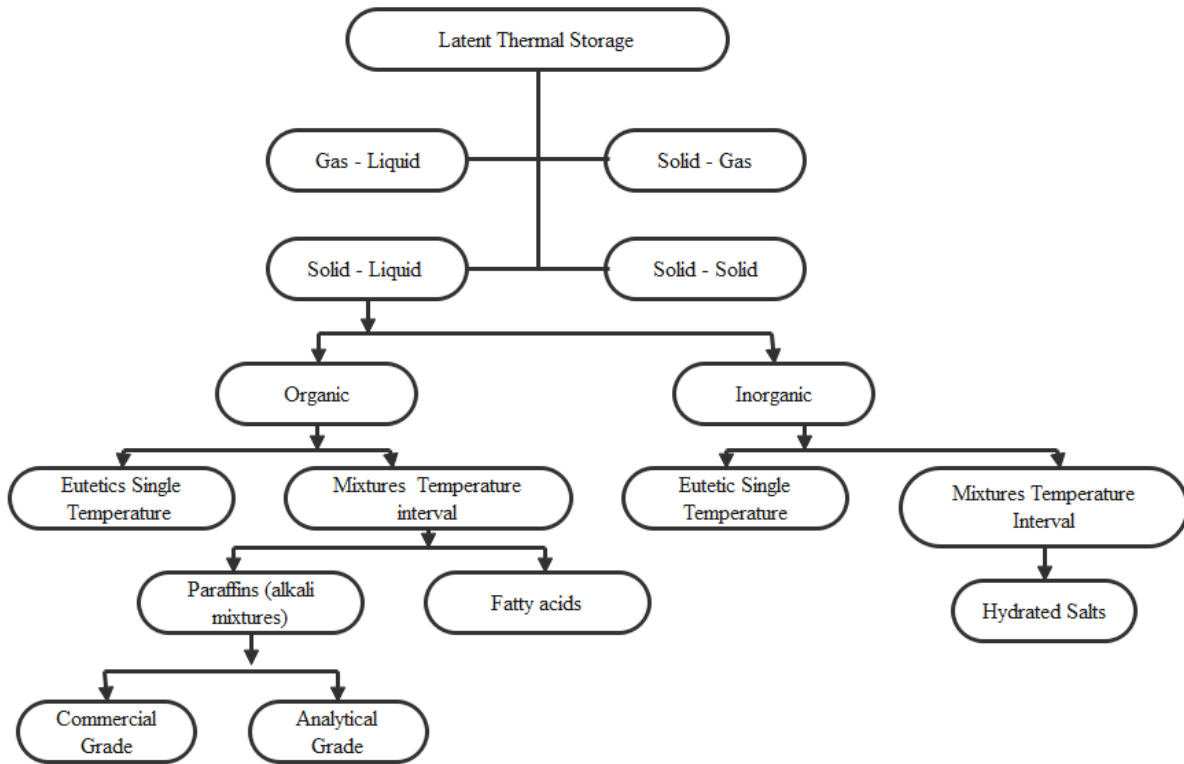


Figure 3: PCMs Classification [7]

Table 1: Typical Values of Inorganic PCMs

PCM Name	Melting Temperature [°C]	Heat of Fusion [kJ/kg]	Thermal conductivity [W/mK]	Density [kg/m ³]
KF·4H ₂ O Potassium fluoride tetrahydrate	18.5	231	n.a.	1447 (liquid, 20°C) 1455 (solid, 18°C)
Mn(NO ₃) ₂ ·6H ₂ O Manganese nitrate hexahydrate	25.8	125.9	n.a.	1738 (liquid, 20°C) 1728 (liquid, 40°C) 1795 (solid, 5°C)
CaCl ₂ ·6H ₂ O Calcium chloride hexahydrate	29.0	190.8	0.540 (liquid, 38.7°C) 1.088 (solid, 23°C)	1562 (liquid, 32°C) 1802 (solid, 24°C) 1710 (solid, 25°C)
CaBr ₂ ·6H ₂ O Calcium bromide hexahydrate	34	115.5	n.a.	1956 (liquid, 35°C) 2194 (solid, 24°C)
Na ₂ SO ₄ ·10H ₂ O Sodium sulphate decahydrate	32.4	254	0.544	1485 (solid)
Na ₂ CO ₃ ·10H ₂ O Sodium carbonate decahydrate	34.2	246.5	n.a.	1442



Na ₂ HPO ₄ ·12H ₂ O orthophosphate dodecahydrate	Sodium	35.5	265	n.a.	1522
Zn(NO ₃) ₂ ·6H ₂ O Zinc nitrate hexahydrate		36.2	146.9	0.464 (liquid, 39.9°C) 0.469 (liquid, 61.2°C)	1828 (liquid, 36°C) 1937 (solid, 24°C) 2065 (solid, 14°C)

n.a.=not available

Table 2: Organic PCMs (typical values)

PCM Name		Temperature [°C]	at of Fusion [kJ/kg]
CH ₃ (CH ₂) ₁₆ COO(CH ₂) ₃ CH ₃	Butyl stearate	19	140
CH ₃ (CH ₂) ₁₁ OH	1-dodecanol	26	200
CH ₃ (CH ₂) ₁₂ OH	1-tetradecanol	38	205
CH ₃ (CH ₂) _n (CH ₃ ...	Paraffin	20-60	200
45%CH ₃ (CH ₂) ₈ COOH	45/55	21	143
55%CH ₃ (CH ₂) ₁₀ COOH	capric-lauric acid		
CH ₃ (CH ₂) ₁₂ COOC ₃ H ₇	Propyl palmitate	19	186

Applications of PCM in Forced Convection

Researchers from several domains have paid considerable interest to forced convection techniques utilising phase change materials (PCM). Phase change materials (PCMs) are useful for improving heat transfer rates and temperature stability because they can store and release thermal energy during phase shifts.

- Phase change materials (PCMs) may release stored energy via the process of forced convection. This characteristic proves to be advantageous in discharging cycles and for the operation of certain cooling or heating devices [8].
- [9] Investigates the Phase change material (PCM) induced convection transfer of heat characteristics Nano emulsions, which possess the advantageous capability of storing substantial amounts of heat while undergoing phase transition with minimal temperature variation.
- [10] proposes the utilization of hybrid cooling systems that integrate forced convection with passive heat sinks based on PCMs have been identified as the best solution for achieving long-term conditioning of high-power electronic equipment over extended periods.
- [11] Involves the numerical modelling of Devices for storing latent thermal energy that incorporate phase-change materials with induced convection. The investigation is limited to systems with annulus and also countercurrent flows.
- [12] Introduces an innovative three-region melting model for conduction- phase-change material (PCM) slurries are used to drive heat transfer. The concept aims to tackle the challenges that emerged during the investigation of heat transfer in PCM slurry flow.

The aforementioned examples demonstrate the many uses of phase change materials (PCM) in forced convection scenarios, including areas such as energy dissipation, temperature regulation in cooling and heating apparatus, heat transmission in electronic devices, as well as energy storage systems.

Applications of PCM in Heat transfer

PCMs have various applications in various sectors, including solar energy, buildings, and vehicles, to minimize greenhouse effects and reduce the need for foreign gasoline. Solar energy is a promising



alternative energy resource, but its reliability may be boosted by storing surplus energy and utilizing it when required. For more than 30 years, PCMs have been explored to reduce heat either lost or gained via walls, ceilings and floors, hence lowering electricity and natural gas usage in buildings [13]. Studies on the practicality of PCMs with vehicle uses are also expanding, since refrigerated vehicles partly alleviate the issue of food denaturation during transportation, but it also results in more costly foods and permanent environmental consequences on living creatures [14]. Overall, PCMs are a viable option for energy management and also environmental protection concerns.

Solar energy

Sun thermal energy is a way of generating thermal power by using sun energy, which gets absorbed by the earth's surface and dissipated at varying rates in the ground. This energy may be transmitted between heating/cooling locations on the ground and in the air. Solar water heaters have grown in popularity during the late 1960s. Since the 1980s, passive systems based on PCMs have been used to store thermal energy [15].

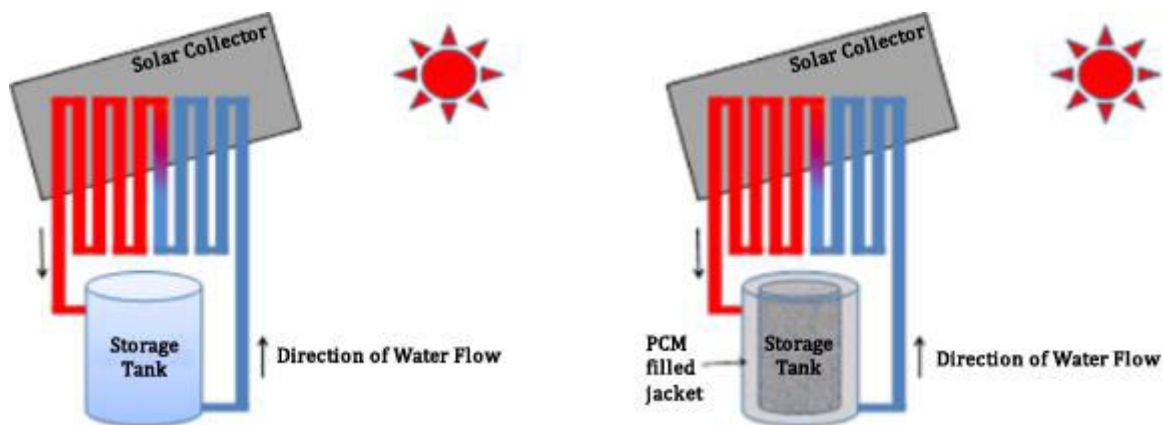


Figure 4: Solar heating system with and without PCM

Building applications

PCMs are flexible equipment used in building with a small temperature range for temperature adjustment, cold or warm storage, along with thermal comfort. By storing available energy through the day and maintaining a suitable temperature in the building, they may efficiently store solar energy against night cold and satisfy heating demand [16].

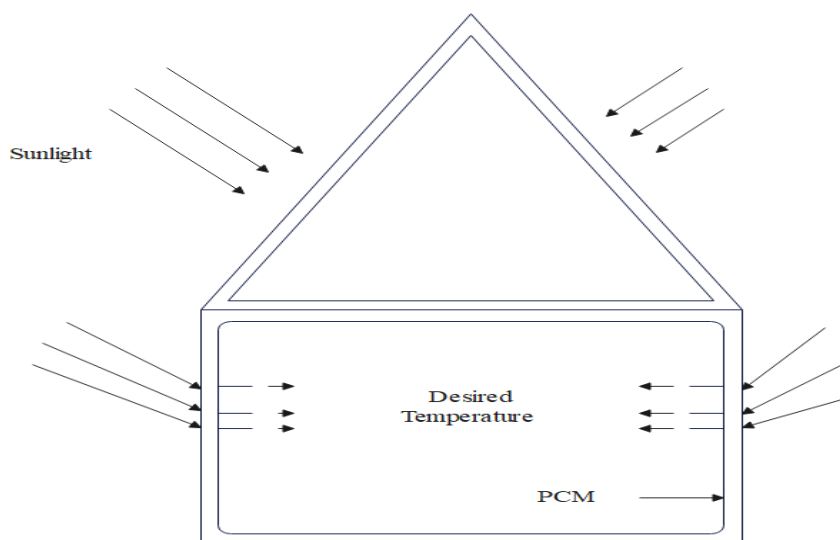


Figure 5: Typical application of PCM in Buildings

Encapsulating polymer-based materials (PCM) within building surfaces can enhance energy storage and minimise energy usage without considerably increasing the weight of building materials. PCM absorbs solar radiation as well as created by humans heat or cold, eliminating temperature fluctuations and ensuring a stable temperature range [17]. Researchers have suggested encapsulating PCM at the Concrete at the macro or micro level, Gypsum out walls board, ceiling, along with floor to produce a stable temperature range. Small quantities of PCM can reduce maximum and minimum peak temperatures, absorb solar energy, and delay external heat load. PCM walls have better heat-insulation performance during charging and discharging processes. PCMs' attributes vary depending on environmental factors, and their usefulness is enhanced when the PCM changes state due to in-wall temperatures [18].

Vehicle Applications

PCMs are being studied for their potential in vehicle applications, particularly in refrigerated trucks and hybrid vehicles. PCMs have been found to Lower peaks heat transfer rates and overall heat flows, possibly resulting in energy savings, pollution reduction, and equipment operating life extension. Paraffin-based PCMs were utilised in refrigerated vehicles to minimise peaks heat transfer rates and overall heat flows. This might lead to energy savings, lower emissions, and longer equipment life. However, because of exothermic electrochemical processes that release energy during discharge, the utilisation of Li-ion batteries for transportation applications offers a difficulty. Researchers have proven this PCM-based thermal management may reduce the requirement for extra cooling systems while increasing available power. Because PCM's latent heat of fusion is really high, it can remove huge amounts of heat, making it a viable alternative for lowering energy consumption and emissions in vehicles [19].

PCM models and computational domains

The incorporation of PCM models and the definition of computational domains are crucial elements in the implementation of numerical simulations for studying heat transfer phenomena involving phase-change materials. The computational domain is the three-dimensional space where the fluid flow takes place. In order to conduct numerical simulations, it is necessary to discretize this domain into a computational grid [20].

Mathematical models for PCM flow and heat transfer

The prediction of phase-change system behaviours poses challenges owing to the intrinsic nonlinearity associated with the movement of user interfaces. This nonlinearity arises from the influence of latent heat, which is both lost and accumulated at the system's boundaries, hence governing the rate of displacement. The following equation, sometimes referred to as the Stefan condition, delineates the aforementioned procedure:

$$\lambda_p \left(\frac{ds(t)}{dt} \right) = k_s \left(\frac{\delta T_s}{\delta T} \right) - k_l \left(\frac{\delta T_l}{\delta t} \right) \quad (4)$$

The surface position, denoted as $s(t)$, is associated with the conductive heat, t , temperature, and λ is the fusion's latent heat. Whether the density is for a solid or a liquid is not specified. S and λ , respectively, indicate the presence of liquid and solid phases.

The boundary' position and velocity in this case are unknown beforehand. Furthermore, because the two phases have different physical characteristics, there may be nonphysical discontinuities in the numerical model issues that must be addressed.

Fixed grid

When the enthalpy approach is used, interface conditions are quickly fulfilled since the equation that governs for the two phases is the identical, creating a mushy transition between the two stages also

making it far easier to tackle the phase-change problem. We stay away from sharp discontinuities in this region since they might cause numerical instability.

Consequently, the model's performance is highly dependent on the mushy zone's discretization thickness and quality. While the actual temperature at a conventional grid point may change over time, problems with transitions between mushy and isothermal phases are easily handled with the enthalpy method [21]. Numerous phase-change issues have been effectively solved using this approach [22]. According to, the enthalpy technique is most suited for common applications [23] and Kotalík [24], given that the numeric scheme at the interface stays constant.

[25] Provides the temperature is shown by the enthalpy function. Conserving energy across a phase-change process for constant thermo physical properties may be described as following (from [5]) regarding the total volumetric enthalpy and temperature:

$$\frac{\partial H}{\partial t} = \nabla [k_k (\nabla T)],$$

(5)

Total volume enthalpy, abbreviated as "H," is the sum of sensible and latent heats:

$$H(T) = h(T) + \rho_l f(T) \lambda$$

(6)

And where

$$h = \int_{T_m}^T \rho_k C_k dT$$

(7)

The percentage of liquid f In the event of an isothermal phase transition

$$f = \begin{cases} 0 & T < T_m \text{ solid,} \\]0, 1[& T = T_m \text{ mushy,} \\ 1 & T > T_m \text{ liquid,} \end{cases}$$

(8)

Using Eqs. (6) And (7), a new form for dimension structure heat transfer in the PCM is developed in both directions may be written:

$$\frac{\partial h}{\partial t} = \frac{\partial}{\partial x} \left(\alpha \frac{\partial h}{\partial x} \right) + \frac{\partial}{\partial y} \left(\alpha \frac{\partial h}{\partial y} \right) - \rho_l \lambda \frac{\partial f}{\partial t}$$

(9)

Where α is the thermal diffusivity

To deal with phase-change difficulties, early Finite variation and also finite-element approaches were employed as numerical methods. Following which, Volume control and finite volume methods were employed [26]. The emergence In the 1970s, the popularity of finite-element along with finite-volume techniques led to their predominance over finite-difference approaches.

Some publications employ a heat capacity technique based on temperature variations that occur intermittently. Instead of using an energy equation based on enthalpy, these models use a one-variable non-linear equation. Here we see the TTM (Temperature Transforming Model) in action. The simulation method is precise, easy to use, and highly effective [27].

Fluid problems are solved by TTM using general continuity and momentum equations. The energy equation differs from the enthalpy formalism by including a temperature-dependent source term.

Developing a means to maintain the point of zero velocity within the solid state phase fundamental challenge of this technique. One of the most basic methods is the switch-off technique (SOM) or its smoother variation, the ramping SOM [28]. These methods set to prevent motion, reduce By adjusting the momentum and also velocity-correction equation coefficients, solid phase velocities may be reduced to zero. Despite a fact that this method is often utilized in phase-change problems, [21] found But when used to mimic convection-controlled solid-liquid phase shift using a TTM model issues, there is a considerable difference. A mushy region assures constant temperature in TTM, whereas velocities were disconnected at the solid-liquid boundary in SOM. Two variants of this method, including a rising speed cutoff, use a mushy zone between the solid and liquid phases to eliminate discontinuities.

The energy equation at the interface can also be rewritten by changing the source term (STM) rather than the correction coefficients for momentum and velocity. Similar to SOM, this approach has a discontinuity at the interface, causing the same issue. Consider using a scaled version of this approach (RSTM). Darcy STM is a kind of ramping STM that has been created for phase-change simulations utilizing the enthalpy technique. [29].

A third option, as proposed by Gartling, is to employ a variable viscosity of the medium (VVM) [30]. This method involves setting high viscosity in the solid phase to stop motion.

Ma and Zhang [21] compared TTM approaches to Okada's [31] experimental results. Ramped SOM and STM were found to perform better, although at a little greater computational cost. They also mentioned a tiny time step leads to poor convection modeling and divergent model solutions.

Adaptive mesh

To accurately simulate melt front physical processes, it is essential that the densities of the model grid adequately encompass the solid-liquid interactions. Other fields of mathematics do not need this level of density. It is normal to modify grid density in local physical computing to increase processing efficiency circumstances. Two basic methods are employed. Local mesh refinement is done using h-method [32]. At each iteration, the model begins with an even grid and also adds or subtracts grid points to achieve accuracy. This strategy is employed in most business codes. This method's key issue is data structure maintenance because the topology and grid points change between time steps.

Finite element analysis uses adaptive methods to improve solution accuracy. The h-method and the r-method are the two most common methodologies. By increasing the amount of nodes and elements and splitting them into regions with high error estimates, the h-method improves the mesh. This method is more flexible and can control error distribution. However, it can be computationally expensive and may suffer from element distortion in large deformation problems. The r-method increases the polynomial order of shape functions within existing elements, improving approximation capabilities without changing the mesh topology. It is more computationally efficient and reduces mesh distortion issues [33].

Lacroix and Voller [34] compared rectangular cavity phase-change model simulation approaches. For a because each material has a different melting temperatures, the fixed grids must be finer, but the A coordinate generator must be used at each stage, which limits moving mesh. Jaluria and Viswanath [35] and Bertrand et al. [36] compared fixed and moving grids. In cases when there is no obvious surface where a liquid turns into a solid, front tracking methods will fail to provide an appropriate simulation. Consequently, enthalpy approaches should be employed in the majority of solidification issues involving regions with solid-liquid interfaces.

The model of first and second law

Some models are created with the express purpose of measuring the second law's impact, while others are tailored to evaluate the first law's efficacy. First law models have their limitations due to their inability to consider the duration of heat storage or extraction, the temperature of heat transportation, and the surrounding environment. The challenges of achieving the most efficient designs and

operations are addressed by second law models. It is the intention of second law models to supplement, not supplant, first law models. How well a thermal energy storage system transforms incoming energy into usable output energy is the primary determinant of its efficiency according to the first law.

$$\eta = \frac{Q_r}{Q_s} \quad (10)$$

Where Q_s is the total heat that the phase-change material absorbs during the thermal preservation process, and Q_r is the total thermal energy that the heat recovery medium has produced during the process. The following equation defines the heat energy storage system's second law efficiency:

$$\psi = \frac{\phi_r}{\phi_s} \quad (11)$$

Numerical methods for simulating PCM heat transfer

The discontinuities caused by the moving interface's nonlinearity and the distinct thermo physical characteristics of the two phases make solving the Stefan problem challenging. Instead than being disregarded in Stefan situations, numerical techniques especially in the face of significant convection, may be a powerful tool for resolving the moving-boundary issue [37]. Front-tracking and fixed-grid methods are the primary techniques used to numerically model phase change problems [38]. The firsts are more accurate, but they can only be used in basic applications and geometries because they are hard to implement. Their fundamental method is to solve the problem at each time step using governing equations by estimating the prior location of the moveable interface. Although the seconds are easier to use and faster, they do not provide the precise location of the shifting boundary.

Front-tracking methods

Three front-tracking strategies that have been effectively employed to handle the In planar geometry, Stefan problems are solved using the variable space grid technique (VSGM), The 'boundary immobilization technique (BIM)' and an 'nodal integral method (NIM)' [39]. The front is tracked in both the BIM and NIM at every period step, but the problem domain is altered to a defined one, reducing the challenges associated with managing the shifting interface. While NIM uses FEM, BIM employs a finite difference method. As opposed to the other two approaches, the VSGM does not convert the domain into a fixed one. As the phase change process progresses, the movable the border is established at the grid's last point at each time step by widening the space width gap [40]. The BIM process is as follows Where the half planes melts at the phase transition temperature and a Dirichlet's border condition exists $T(x = 0, t > 0) = T_1$, with $T_1 > T_m$:

Results from the domain transformation are:

$$x^* = \frac{x}{s}, T^*(x^*, t) = T(x, t) \quad (12)$$

In the fixed domain, a solid and an interface may be combined to make one: $0 < x^* < 1$:

$$s^2 \frac{\partial^2 T^*}{\partial T} = \frac{\partial^2 T^*}{\partial x^{*2}} + x^* s \frac{ds}{dt} \frac{\partial T^*}{\partial x^*} \quad (13)$$

The boundaries are expressed as follows:

$$T^*(x^* = 0, t) = T_1, T^*(x = 1, t) = 0 \quad (14)$$



$$s \frac{ds}{dt} = -St \frac{\partial T^*}{\partial x^*}; \quad x^* = 1$$

(15)

Where the $St = \rho c_s \frac{T_m - T_1}{L}$ is Stefan's phone number. The discretization procedure of equation's implicit central finite-differential. (13) T^* and it is explicit in s :

$$a_i^{(k+1)} T_{i-1}^{(k+1)} + b_i^{(k+1)} + T_i^{(k+1)} + c_i^{(k+1)} T_{i+1}^{(k+1)} = \left(s^{(k)} \right)^2 T_i^{(k)}$$

(16)

Where,

$$a_i^{(n+1)} = \frac{\Delta t}{(\Delta x)^2} \left[\frac{\Delta x}{2} x_i s^{(k)} \left(\frac{ds}{dt} \right)^{(k)} - 1 \right]$$

(17)

$$b_i^{n+1} = \left(s^n + 2 \frac{\Delta t}{(\Delta x)^2} \right)$$

(18)

$$c_i^{n+1} = -a_i^{k+1} - 2 \frac{\Delta t}{(\Delta x)^2}$$

(19)

$$\left(\frac{ds}{dt} \right) = \frac{St}{s^n} (4T_{N-1}^n - T_{N-2}^n)$$

(20)

Equation (16) is solved to get the temperature profile is changed at every stage of the process, as well as the shifting locations interface are modified using the specific equation that follows:

$$s^{n+1} = s^n + \left(\frac{ds}{dt} \right)^{(n)} \Delta t$$

(21)

The nodal point i is represented by the subscript i , while its adjacent points to the left and right are marked by the subscripts $i+1$ and $i-1$, respectively. In this case, $n + 1$ denotes the current time-level, while n represents the prior time-level. Since N is the last node in the modified grid that stands in for the interface, the two nodes before it are $N - 1$ and $N - 1$. Although Crank's extensive work uses this approach in a more general setting with two phases, it zeroes in on the one-phase Stefan Problem as its particular case study. The domain transformation, however, will result in a singularity if the phase change front is initially situated at the origin at the first time step. The precise analytical solution currently accessible can serve as the initial time law for the interface of the semi-infinite wall. However, for complex geometries, an estimation of the solution is necessary as the exact solution does not exist.

Arbitrary Lagrangian Eulerian method

Geometries can be allowed to deform during a transient using methods that can be found in commercial software such as Comsol or Ansys. Consequently, if both phases are present at time $t=0$, these techniques can be used to simulate solidification or melting [41]. The entire geometry is actually split into two domains: a liquid and a solid one. Because of a moving boundary dividing them, these domains distort as the PCM melts or solidifies. The outside boundaries are given zero normal displacements if volume fluctuations are ignored, and the moving boundary's normal velocity is calculated using the Stefan condition:



$$v_n \cdot \Omega = (q_l - q_s) / (L^* \rho) \quad (22)$$

Where n denotes the normal component, the moving boundary is denoted by the subscript Ω , and the heat flows between the liquid along with solid domains internal boundary are represented by the letters q_l and q_s , respectively.

Deformations are defined by the velocity of the interface and the assigned displacements. There are four smoothing methods that can be used to calculate the deformation: Laplace, Winslow, Hyperplastic, and Yeah. The differential equation given below can be solved using the Laplace smoothing method:

$$\frac{\partial^2 x}{\partial X^2} + \frac{\partial^2 y}{\partial Y^2} + \frac{\partial^2 z}{\partial Z^2} = 0 \quad (23)$$

Where x , y , and z are the undeformed coordinates of the mesh and X , Y , and Z represent its deformed coordinates. Physical quantities are related to fixed places in space, hence the Eulerian description is unable to deal with shifting boundaries. Consequently, in these circumstances, an arbitrary Lagrangian Eulerian approach will be applied. Actually, it enables the mesh and space to have two distinct coordinate systems defined. The domain boundaries of a mesh coordinate system are fixed, and the mesh coordinates are translated into spatial coordinates via a map. These coordinate systems initially overlap, however the mesh coordinate system varies when the domain begins to deform. A good remeshing is required to prevent several stability issues since a heavily deformed mesh might cause the map to mesh to spatial locations becomes skewed. When a predefined threshold is reached, the simulations stop and the grid is regenerated. The distorting effect of the grid reaching a pretty a high price or the mesh's quality being inadequate low are two instances of remesh situations. The spatial system and the new mesh system of coordinates coincide once more following the remeshing [42].

Fixed grid methods

It is expected in fixed grid approaches that a mushy zone is specified instead of a zero-thickness front where the phase transition takes place. This makes the situation simpler because the discontinuities brought about by the interface's presence are eliminated by the mushy region which lies between the stages. The energy formula for the major conduction/diffusion phase change is as follows [43]:

$$\frac{\partial H}{\partial t} = \nabla(k \nabla T) \quad (24)$$

where k is the conductivity and H is the total volumetric enthalpy, which is a combination of latent and visible heat contributions.

$$H = h_0 + \int_{T_0}^T \rho c dT + f L \quad (25)$$

In the instance of an adiabatic phase transition, the fraction's value of liquid. They or f , is determined by a function that operates piecewise and may be represented as follows:

$$f = \begin{cases} 0 & T < T_m \\]0, 1[& T = T_m \\ 1 & T > T_m \end{cases} \quad (26)$$



The three groups of fixed grid methods are then as follows: enthalpy methods, apparent heat capacity methods, and source based approaches.

Enthalpy method

By first determining the enthalpy the problem of temperature was indirectly solved through the at each time step enthalpy technique. Equation (24), discretized with Finite-Volumes, is as follows [44]:

$$H_p^{n+1} = H_p^n + \sum_{nb} a_{nb} T_{nb}^{n+1} + a_p T_p^{n+1} \tag{27}$$

The discretization coefficients are represented by the letters a's. The symbol denotes a node between point p along with its neighbors subscripts p and nb, respectively, while the actual and old time-steps are indicated by the up scripts n + 1 and n, respectively.

In order to prevent discontinuities like those found in equation (27), As a result, this the temperature enthalpy is connected to equation (28) equation that has been opportunisticly smoothed if the phase shift is isothermal.

Since the enthalpy H_p^{n+1} varies on the temperature T_{nb}^{n+1} , the system is consequently non-linear and needs to be solved using iterative techniques like the Newton ones.

$$T_p = \left\{ \begin{array}{ll} H_p / C_s & T \leq T_m - \Delta T \\ \frac{H_p + \left[\frac{c_1 - c_2}{2} + \frac{L}{2\Delta T} \right] (T_m - \Delta T)}{\frac{c_1 - c_2}{2} + \frac{L}{2\Delta T}} & T_m - \Delta T < T < T_m + \Delta T \\ \frac{H_p - (C_s - C_t) T_m - L}{C_t} & T \geq T_m \end{array} \right. \tag{28}$$

Where the phase transition temperature interval (ΔT) is divided in half. Due to the nonlinearity of the (27), the enthalpy technique is more stable than the others, but it is more complex to implement [45].

Method for apparent heat capacity

In an apparent heat capacity approach, it is written as follows:

$$C_{app} \frac{\partial T}{\partial t} = \nabla [k \nabla T] \tag{29}$$

Where C_{app} , This is the phase-change material's apparent heat capacity as well as is defined as a time derivatives of total the volumetric enthalpy:

$$C_{app} \frac{\partial T}{\partial t} = C(T) + L * \delta(T - T_m) \tag{30}$$

Where the temperature derivative of the liquid fraction is represented by δ , the Dirac-delta. According to Bonacina et al. [25], the Dirac function's associated challenges can be eliminated by substituting a smoothed function that assumes finite values in the interval larger than zero $T_m - \Delta T < T < T_m + \Delta T$. where half of the mushy zone temperature range is represented by ΔT , much like in the enthalpy technique. The answer to the smoothed issue is similar to the original one when it approaches zero. However, from a numerical perspective, it shouldn't be too little because that would result in convergence errors. The definition of approximate heat capacity is:



$$C^*(T) = \begin{cases} C_s(T), & T < T_m - \Delta T \\ C_l(T), & T > T_m + \Delta T \end{cases}$$

(31)

While for $T_m - \Delta T < T < T_m + \Delta T$ it is unknown, but its integral is defined as follows:

$$\int_{T_m - \Delta T}^{T_m + \Delta T} C^*(T) dT = L + \int_{T_m - \Delta T}^{T_m} C_s(T) dT + \int_{T_m}^{T_m + \Delta T} C_l(T) dT$$

(32)

Different functions can be used to estimate the heat capacity in the mushy zone (Fig. 7), but they must be defined in a way that ensures the validity of equation (32). Assuming that C_s and C_l are temperature independent, this interval's estimated apparent heat capacity can be stated as:

$$C^*(T) = \frac{L}{2\Delta T} + \frac{C_s + C_l}{2}$$

(33)

It follows that the change in the liquid fraction f is linear in the mushy area. Then, Total Enthalpy is a piecewise-linear function, and step functions are used to estimate the Dirac delta, and therefore its apparent heat capacity. Another method that is frequently utilised in textbooks is defining the liquid fractional as an error functional that varies with temperature. In that case, a normal distribution over the soft zone can be used to get a rough idea of the Dirac delta [46]:

$$\frac{\partial f}{\partial t} = \frac{\sigma}{\sqrt{\pi}\Delta T} e^{-\left[\frac{\sigma^2(T-T_m)^2}{\Delta T^2}\right]}$$

(34)

Where $\text{erf}(\sigma) = 1 - \lambda$ is achieved by selecting σ . where λ is a small enough value. According to the normal distribution approximation, the following definition of the mushy zone, in which the solid and liquid states have the same heat capacity, $C_s = C_l = C_{sl}$, is given:

$$C^*(T) = C_{sl} + L \frac{\sigma}{\sqrt{\pi}\Delta T} e^{-\left[\frac{\sigma^2(T-T_m)^2}{\Delta T^2}\right]}$$

(35)

In 1978 and 1979, Lemmon [47] and Morgan et al. [48] introduced a spatial and temporal averaging method for statistically evaluating Heat capacity that can be seen. Heat capacity as perceived is the same in both techniques is calculated as the numerical mean of the enthalpy time-derivative, $\partial H / \partial t$.

Spatial averaging:

$$C^*(T) = \sqrt{\frac{\nabla H \nabla H}{\nabla T \nabla T}}$$

(36)

In which each spatial derivative is assessed at the same time step. It can be put into practice using both explicit and implicit time methods.

Average time: The time-scheme determines how time-averaging is expressed. The formulation for an explicit scheme with two time levels is:

$$C^*(T^{(k)}) = \frac{H^{(k)} - H^{(k-1)}}{T^{(k)} - T^{(k-1)}}$$

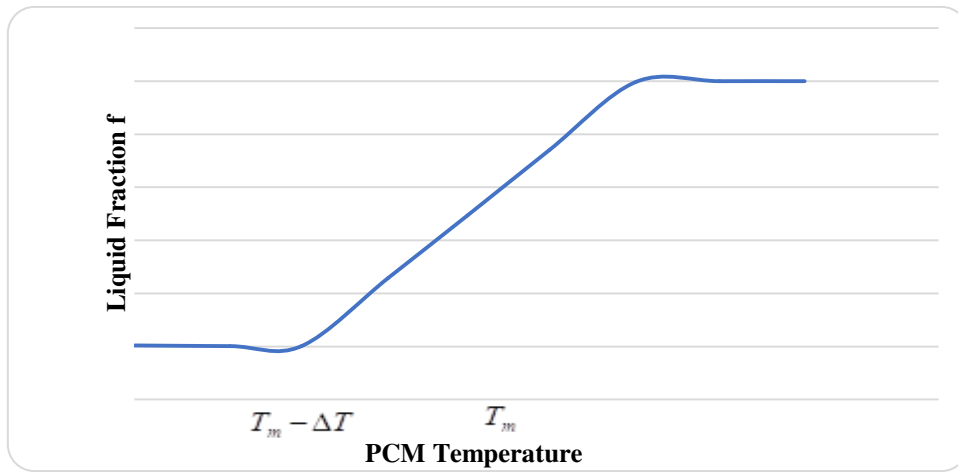
(37)

To prevent the discontinuities, it is also necessary to incorporate a smoothed conductivity. It is typically believed that k^* would vary linearly in the interval $T_m - \Delta T < T < T_m + \Delta T$. In the event where k_s and k_l are temperature independent, the smoothed conductivity can be characterized as follows:

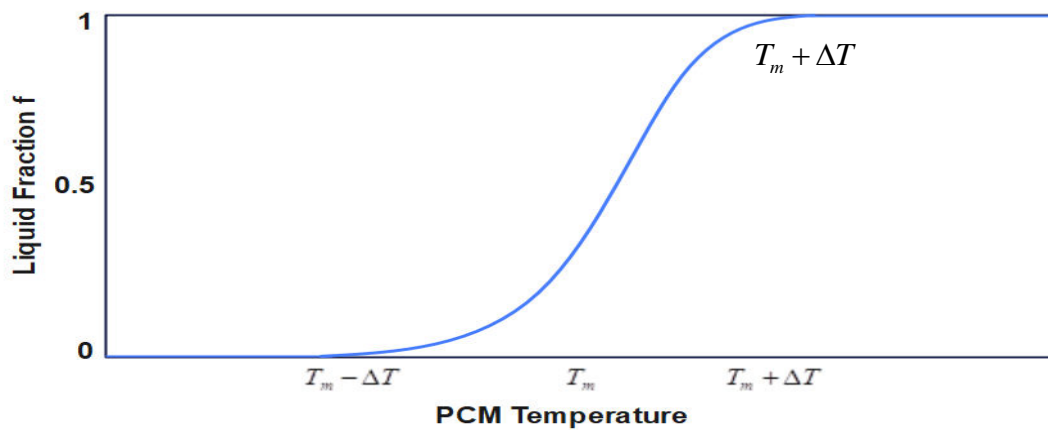
$$k^* = \begin{cases} k_s & T \leq T_m - \Delta T \\ k_s + \frac{k_l - k_s}{2\Delta T} [T - (T_m - \Delta T)] & T_m - \Delta T < T < T_m + \Delta T \\ k_l & T \geq T_m + \Delta T \end{cases} \quad (38)$$

After the approximations, eq. (29) becomes:

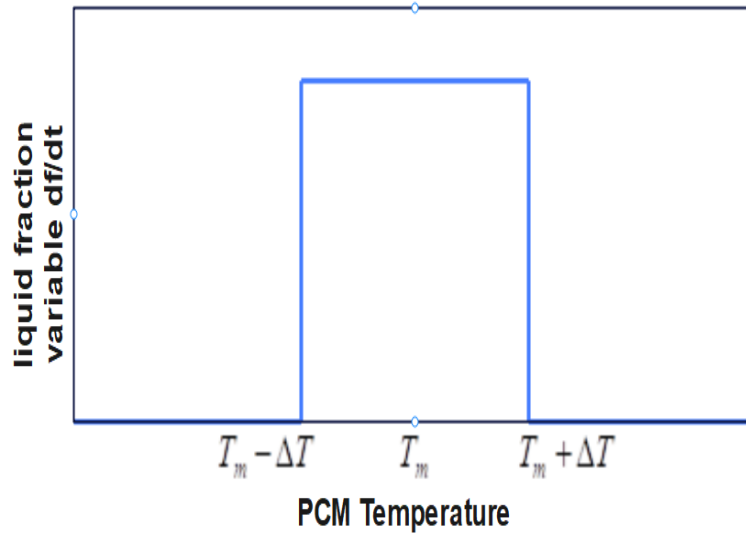
$$C^*(T) \frac{\partial T}{\partial T} = \Delta [k^*(T) \Delta T] \quad (39)$$



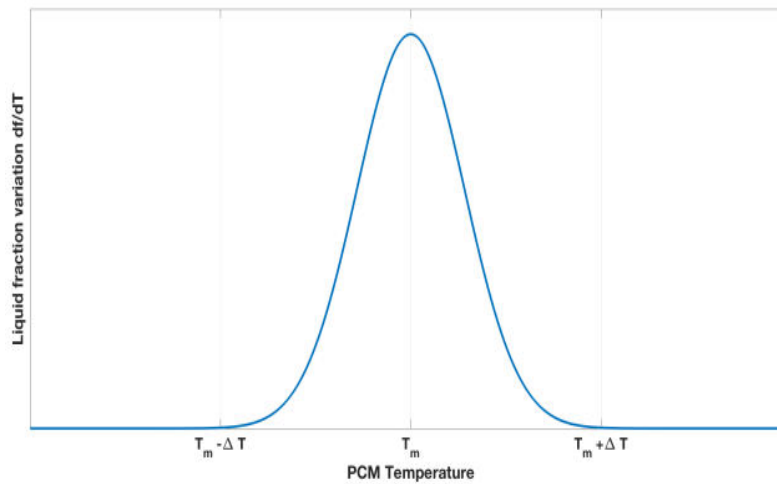
(A) linear ratio of liquid to temperature



(B) Liquid fraction as a temperature error function



(C) Step function-based approximation of Dirac delta



(C) Normal distribution in the Dirac Delta approximation

Figure 6: Approximations of the mushy zone's liquid fraction and its derivative

Source based method

Assuming constant thermo physical parameters, In source-based approaches, the heat that is latent release, which is viewed as a heat source, may be stated as follows:

$$\rho c \frac{\partial T}{\partial t} = k \nabla^2 T - L \frac{\partial f}{\partial t} \tag{40}$$

When discretized using the finite volume approach, it becomes [22]:

$$\left[a_p + (\rho c V)_p \right] T_p^{m+1} = (\rho c V)_p T_p^m + \sum_{nb} a_{nb} T_{nb}^{m+1} + (\rho L V)_p \left[f_p^{old} - f_p^m \right] \tag{41}$$

When V denotes the total volume for the cell associated with node p, and the subscripts p as well as nb signify the node point p along with its neighbours, and the up scripts m and also old define the current and iteration level, as well as the prior time-step, and so forth. After each iteration, the liquid percentage is updated and the heat field is calculated iteratively as follows:

$$f_p^{m+1} = f_p^m + \lambda \Delta$$

(42)

Where Δ is a correction term and λ is a factor of under-relaxation. To restrict the range of possible values in $[0,1]$, an undershoot/overshoot adjustment is applied to the up to date liquid fraction. After convergence, the iterative calculation for another time period is repeated, beginning at $f_0^p = f_{old}^p$ [49]. Several writers used various methods to compute the adjustment term. Cross et al. suggested, for instance, that it be calculated directly using the temperature-dependent liquid fraction function [50]:

$$\Delta = F(T_p^{m+1}) - f_p^m$$

(43)

Whereas The dependent on temperature liquid fraction is denoted by $F(T)$. This function has the ability to take on a variety of forms, but in the event of an isothermal phase shift, it is necessary to approximate and smooth it in order to prevent discontinuities—a process that is analogous to the enthalpy approach. Determining the ideal value for the under-relaxation parameter is the primary challenge associated with this approach.

Heat transfer enhancement technologies

The enhancement Many tactics, such as the use of lower-density substances, porous materials, encapsulating technologies, fins, heat pipes (HPs), transmitted systems of storage, and direct transfer of heat techniques, may be applied to latent heat energy storage to improve heat transmission. The most popular techniques are to use longer surfaces or to combine various phase change materials (PCMs) with differing melting temperatures. Heat flow may be enhanced in two distinct ways: through expanding the surface area utilised for the transfer of heat or through improving the heat-transfer medium's material storage substance's thermal characteristics [16]. Some of them are discussed below.

Low-density materials

Experimental investigations have been conducted to assess the efficacy of using Metal constructions with high thermal conductivity are utilised to facilitate heat transfer transmission in thermal storage (TES) solutions. Metal framework have high densities, which causes them to gravitate to the bottom of a container containing phase-change material (PCM). Carbon fibres are considered to be superior alternatives to other materials owing to their lower densities as well as thermal conductivities, making a variety of Phase Change Materials (PCMs) compatible with them [51]. [52] Carbon cloths and brushes increased effective thermal conductivities by a factor of two. [53] High thermal conductivity carbon fibres embedded in paraffin PCMs have been shown to improve overall thermal conductivity in heat storage devices.[54] Found that composite PCM fibers enhanced heat diffusion. [55] Discovered that transient heat response within carbon brush/noctadecane composite improved satisfactorily. [56] Found that embedding graphite nanofiber (GNF) into paraffin-based PCMs reduces solidification time and enhances TES.

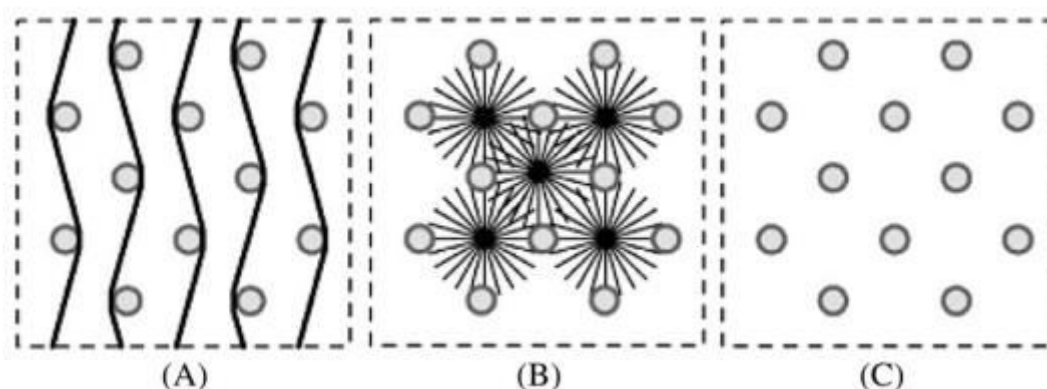


Figure 7: Use of carbon fibers to enhance heat transfer: A, fiber cloth; B, fiber brush; C, no carbon fiber

Porous materials

Porous materials in polymer composite materials (PCMs) enhance thermal conductivity, improving the Low-temperature thermal performance [57]. Paraffin/expanded graphite (EG) composites can incorporate more carbon, increasing Thermal conductivities were increased to 81.2%, 136.3%, 209.1%, and also 272.7%, respectively. However, EG's structural discontinuity makes heat transfer difficult [58]. [59] Salt was used as a PCM to investigate graphite behaviour in conjunction with closed and open pores. They discovered that their graphite matrix restricts fusion expansion volumes, resulting in higher pressure in pores. This causes a gradual rise in melting point of salt and decrease in latent heat, indicating that energy is used to heat the material. [60] studied the usage of metal foams as well as EG to enhance heat conductivity transmission of PCMs. They discovered that both greatly accelerated the rate of heat transmission, although Figure 9 illustrates that metal foams performed better than EG. The reason for this is that heat can go from EG to PCMs more readily because metal foams have a matrix that is far more continuous than EG's structures.

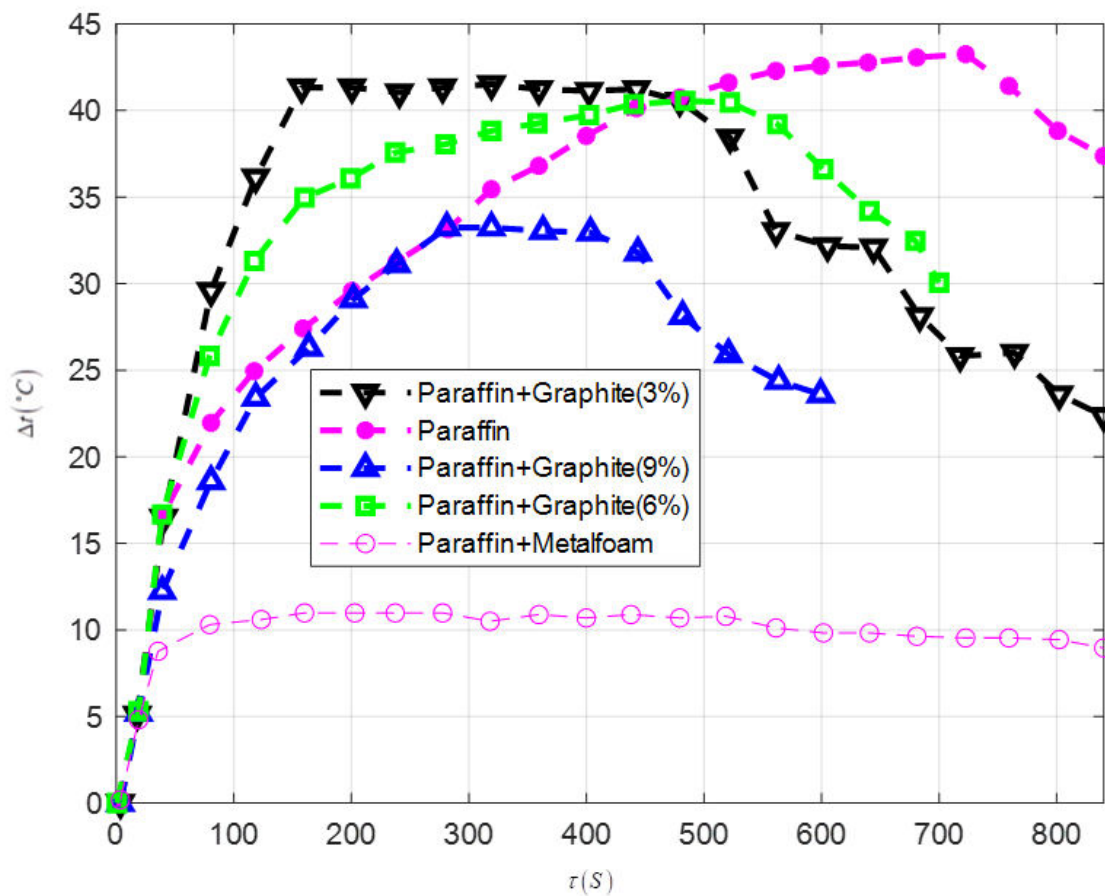


Figure 8: Temperature differences (Δt) between metal foams and EG

Metal matrices

Enhancing because the matrix's limited porosity impedes liquid movement via PCM as well as spontaneous convection. Porosity along with cell size are two properties of a matrix with holes that represent the percentage of volume that the PCM will take up occupy and the pore size measured in pores per inch, respectively. [61] Found that for the first parameter, the matrix's conductivity and porosity both affect how well it performs. Increased performance enhancement is the outcome of a higher effective thermal conductivity caused by low porosity values. Because the matrix's limited porosity impedes liquid movement via PCM as well as spontaneous convection, a reduction in porosity has caused the opposite effect.



Silver, copper, gold, and aluminium are the metals with the greatest thermal conductivity, making them a preferred choice for LHS systems' metal matrix manufacture. The traits they possess are listed in Table 3. The most widely used metals are copper and aluminium because they are less expensive than gold and silver. EG is not as feasible as steel wool in terms of improving PCMs' thermal conductivity. It cannot be compacted as well as graphite, though. Two methods for improving the heat transfer inside a PCM are depicted in Figure 10.



Figure 9: B) Lessing rings made of aluminium and (A) stainless steel

Table 3: Metals that have excellent thermal conductivity

Metal	Melting Point, °C	Specific Heat, J/(kg·K)	Thermal Conductivity, W/(m·K)	Density, kg/m ³
Silver	961.8	237	429.1	10,490
Copper	1084.7	381	387.5	8,978
Gold	1064.5	129	401.2	19,300
Aluminium	660.1	910	237.1	2,800
Nickel	1450.1	440	90.2	8,910

Conclusion

Optimal heat transmission in forced convection settings is the focus of this computational investigation of Phase Change Materials (PCMs). An improved understanding of the complex mechanisms that are involved in increasing the efficiency of heat transmission is one of the contributions that this work produces. Through a comprehensive analysis of several phase change material (PCM) models and computational domains, this research delves into the intricate aspects of heat transfer enhancement. Additionally, a detailed examination of numerical techniques that include Front-tracking and fixed grid methodology is also included. In addition, the research investigates methods that are designed to improve heat transmission. These methods include the insertion of materials that have a low density, porous materials, and metal matrices. These methods shed light on creative possibilities for optimising applications that include forced convection. These findings highlight the importance of adding phase change materials (PCMs) and advanced numerical approaches into heat transfer systems in order to improve their efficiency and ensure their long-term viability. The ramifications of these findings resonate across a variety of areas, including the utilisation of solar energy, applications in building technology, and developments in automobile technology. This highlights the far-reaching influence that adopting PCMs for increased heat transfer performance can have.

References

1. F. Convection, H. Transfer, and F. Convection, "Mixed Convection Heat Transfer - 1993," *Am. Soc. Mech. Eng. Heat Transf. Div. HTD*, vol. 247, pp. 1–86, 1993.
2. B. Pause, "Phase change materials and their application in coatings and laminates for textiles," in *Smart Textile Coatings and Laminates: A volume in Woodhead Publishing Series*





- in *Textiles*, Woodhead Publishing Limited, 2010, pp. 236–250. doi: 10.1533/9781845697785.2.236.
3. L. Xie, L. Tian, L. Yang, Y. Lv, and Q. Li, “Review on application of phase change material in water tanks,” *Adv. Mech. Eng.*, vol. 9, no. 7, p. 1687814017703596, Jul. 2017, doi: 10.1177/1687814017703596.
 4. N. Patil and S. Karale, “Design and Analysis of Phase Change Material based thermal energy storage for active building cooling: a Review,” *Int. J. Eng. Sci. Technol.*, vol. 4, no. 06, pp. 2502–2509, 2012.
 5. L. G. Socaciu, “Thermal energy storage with phase change material,” *Leonardo Electron. J. Pract. Technol.*, vol. 11, no. 20, pp. 75–98, 2012, doi: 10.1201/9780367567699.
 6. A. Heinz and W. Streicher, “Application of PCM and PCM-Slurries for Thermal Energy Storage,” in *In 10th International Thermal Energy Storage*,
 7. Khalid Almadhoni and Sabah Khan, “A Review - An Optimization of Macro-encapsulated Paraffin used in Solar Latent Heat Storage Unit,” *Int. J. Eng. Res.*, vol. V5, no. 01, pp. 729–736, 2016, doi: 10.17577/ijertv5is010294.
 8. M. Kolacek and S. Sehnalek, “Heat Transfer by Forced Convection from a Vertical PCM Plate,” vol. 11, pp. 56–61, 2016.
 9. R. Anderson, M. Kawaji, K. Togashi, and R. Ramnanan-Singh, *Forced Convection Heat Transfer of a Phase Change Material (PCM) Nanoemulsion*. 2013. doi: 10.1115/HT2013-17810.
 10. G. Righetti, C. Zilio, L. Doretta, G. A. Longo, and S. Mancin, “On the design of Phase Change Materials based thermal management systems for electronics cooling,” *Appl. Therm. Eng.*, vol. 196, p. 117276, 2021, doi: <https://doi.org/10.1016/j.applthermaleng.2021.117276>.
 11. Y. Cao, A. Faghri, and A. Juhasz, “A PCM/forced convection conjugate transient analysis of energy storage systems with annular and countercurrent flows,” *J. Heat Transfer*, vol. 113, no. 1, pp. 37–42, 1991, doi: 10.1115/1.2910548.
 12. C. Eunsoo, Y. I. Cho, and H. G. Lorsch, “Forced convection heat transfer with phase-change-material slurries: Turbulent flow in a circular tube,” *Int. J. Heat Mass Transf.*, vol. 37, no. 2, pp. 207–215, 1994, doi: [https://doi.org/10.1016/0017-9310\(94\)90093-0](https://doi.org/10.1016/0017-9310(94)90093-0).
 13. R. Aridi and A. Yehya, “Review on the sustainability of phase-change materials used in buildings,” *Energy Convers. Manag. X*, vol. 15, p. 100237, 2022, doi: <https://doi.org/10.1016/j.ecmx.2022.100237>.
 14. J. Jaguemont, N. Omar, P. Van den Bossche, and J. Mierlo, “Phase-change materials (PCM) for automotive applications: A review,” *Appl. Therm. Eng.*, vol. 132, pp. 308–320, 2018, doi: <https://doi.org/10.1016/j.applthermaleng.2017.12.097>.
 15. A. Kumar, A. Saxena, S. D. Pandey, and S. K. Joshi, “Design and performance characteristics of a solar box cooker with phase change material: A feasibility study for Uttarakhand region, India,” *Appl. Therm. Eng.*, vol. 208, p. 118196, 2022, doi: <https://doi.org/10.1016/j.applthermaleng.2022.118196>.
 16. I. Sarbu and A. Dorca, “Review on heat transfer analysis in thermal energy storage using latent heat storage systems and phase change materials,” *International Journal of Energy Research*, vol. 43, no. 1, pp. 29–64, 2019. doi: 10.1002/er.4196.
 17. M. Zare and K. S. Mikkonen, “Phase Change Materials for Life Science Applications,” *Adv. Funct. Mater.*, vol. 33, no. 12, 2023, doi: 10.1002/adfm.202213455.
 18. Z. Liu *et al.*, “A review on macro-encapsulated phase change material for building envelope applications,” *Build. Environ.*, vol. 144, pp. 281–294, 2018, doi: <https://doi.org/10.1016/j.buildenv.2018.08.030>.
 19. M. Ahmed, O. Meade, and M. A. Medina, “Reducing heat transfer across the insulated walls of refrigerated truck trailers by the application of phase change materials,” *Energy Convers. Manag.*, vol. 51, no. 3, pp. 383–392, 2010, doi: <https://doi.org/10.1016/j.enconman.2009.09.003>.
 20. W. Choopakdee, P. Prasitchoke, A. Shotipruk, and P. Ponpesh, “Computational Fluid Dynamics Modeling for Chromatographic Purification of Free Lutein,” in *24 European Symposium on Computer Aided Process Engineering*, vol. 33, J. J. Klemeš, P. S. Varbanov, and P. Y. B. T.-C. A. C. E. Liew, Eds., Elsevier, 2014, pp. 1393–1398. doi:





- <https://doi.org/10.1016/B978-0-444-63455-9.50067-2>.
21. Z. Ma and Y. Zhang, "Solid velocity correction schemes for a temperature transforming model for convection phase change," *Int. J. Numer. Methods Heat Fluid Flow*, vol. 16, no. 2, pp. 204–225, 2006, doi: 10.1108/09615530610644271.
 22. B. Nedjar, "An enthalpy-based finite element method for nonlinear heat problems involving phase change," *Comput. Struct.*, vol. 80, no. 1, pp. 9–21, 2002, doi: 10.1016/S0045-7949(01)00165-1.
 23. L. W. J. R. Kuttler, Hunte, "The Enthalpy Method for Heat Conduction Problems With Moving Boundaries," *J. Heat Transfer*, vol. 111, no. May 1989, pp. 239–242, 2017.
 24. P. Kotalík, "A numerical solution of the Stefan problem," *Czechoslov. J. Phys.*, vol. 46, no. 9, pp. 793–801, 1996, doi: 10.1007/BF01742450.
 25. V. R. Voller, "FAST IMPLICIT FINITE-DIFFERENCE METHOD FOR THE ANALYSIS OF PHASE CHANGE PROBLEMS," *Numer. Heat Transf. Part B Fundam.*, vol. 17, no. 2, pp. 155–169, Jan. 1990, doi: 10.1080/10407799008961737.
 26. C. Bonacina, G. Comini, A. Fasano, and M. Primicerio, "Numerical solution of phase-change problems," *Int. J. Heat Mass Transf.*, vol. 16, no. 10, pp. 1825–1832, 1973, doi: [https://doi.org/10.1016/0017-9310\(73\)90202-0](https://doi.org/10.1016/0017-9310(73)90202-0).
 27. Q. T. Pham, "A fast, unconditionally stable finite-difference scheme for heat conduction with phase change," *Int. J. Heat Mass Transf.*, vol. 28, no. 11, pp. 2079–2084, 1985, doi: 10.1016/0017-9310(85)90101-2.
 28. M. Yang and W. Q. Tao, "NUMERICAL STUDY OF NATURAL CONVECTION HEAT TRANSFER IN A CYLINDRICAL ENVELOPE WITH INTERNAL CONCENTRIC SLOTTED HOLLOW CYLINDER," *Numer. Heat Transf. Part A Appl.*, vol. 22, no. 3, pp. 289–305, Oct. 1992, doi: 10.1080/10407789208944769.
 29. A. D. Brent, V. R. Voller, and K. J. Reid, "ENTHALPY-POROSITY TECHNIQUE FOR MODELING CONVECTION-DIFFUSION PHASE CHANGE: APPLICATION TO THE MELTING OF A PURE METAL," *Numer. Heat Transf.*, vol. 13, no. 3, pp. 297–318, Apr. 1988, doi: 10.1080/10407788808913615.
 30. C. K. Chun and S. O. Park, "A fixed-grid finite-difference method for phase-change problems," *Numer. Heat Transf. Part B Fundam.*, vol. 38, no. 1, pp. 59–73, 2000, doi: 10.1080/10407790050131561.
 31. M. Okada, "Analysis of heat transfer during melting from a vertical wall," *Int. J. Heat Mass Transf.*, vol. 27, no. 11, pp. 2057–2066, 1984, doi: [https://doi.org/10.1016/0017-9310\(84\)90192-3](https://doi.org/10.1016/0017-9310(84)90192-3).
 32. M. Ainsworth and J. T. Oden, "A posteriori error estimation in finite element analysis," *Comput. Methods Appl. Mech. Eng.*, vol. 142, no. 1, pp. 1–88, 1997, doi: [https://doi.org/10.1016/S0045-7825\(96\)01107-3](https://doi.org/10.1016/S0045-7825(96)01107-3).
 33. Z. Tan, K. M. Lim, and B. C. Khoo, "An adaptive mesh redistribution method for the incompressible mixture flows using phase-field model," *J. Comput. Phys.*, vol. 225, no. 1, pp. 1137–1158, 2007, doi: 10.1016/j.jcp.2007.01.019.
 34. M. Lacroix and V. R. Voller, "FINITE DIFFERENCE SOLUTIONS OF SOLIDIFICATION PHASE CHANGE PROBLEMS: TRANSFORMED VERSUS FIXED GRIDS," *Numer. Heat Transf. Part B Fundam.*, vol. 17, no. 1, pp. 25–41, Jan. 1990, doi: 10.1080/10407799008961731.
 35. R. Viswanath and Y. Jaluria, "A COMPARISON OF DIFFERENT SOLUTION METHODOLOGIES FOR MELTING AND SOLIDIFICATION PROBLEMS IN ENCLOSURES," *Numer. Heat Transf. Part B Fundam.*, vol. 24, no. 1, pp. 77–105, Jul. 1993, doi: 10.1080/10407799308955883.
 36. O. Bertrand *et al.*, "Melting driven by natural convection a comparison exercise: First result," *Int. J. Therm. Sci.*, vol. 38, no. 1, pp. 5–26, 1999, doi: 10.1016/S0035-3159(99)80013-0.
 37. A. Sharma, V. V. Tyagi, C. R. Chen, and D. Buddhi, "Review on thermal energy storage with phase change materials and applications," *Renew. Sustain. energy Rev.*, vol. 13, no. 2, pp. 318–345, 2009.
 38. J. A. Mackenzie and M. L. Robertson, "The Numerical Solution of One-Dimensional Phase Change Problems Using an Adaptive Moving Mesh Method," *J. Comput. Phys.*, vol. 161, no.





- 2, pp. 537–557, 2000, doi: <https://doi.org/10.1006/jcph.2000.6511>.
39. J. Caldwell and Y. Y. Kwan, “Starting solutions for the boundary immobilization method,” *Commun. Numer. Methods Eng.*, vol. 21, no. 6, pp. 289–295, Jun. 2005, doi: <https://doi.org/10.1002/cnm.747>.
40. N. Sadoun, E.-K. Si-Ahmed, P. Colinet, and J. Legrand, “On the boundary immobilization and variable space grid methods for transient heat conduction problems with phase change: Discussion and refinement,” *Comptes Rendus Mécanique*, vol. 340, no. 7, pp. 501–511, 2012, doi: <https://doi.org/10.1016/j.crme.2012.03.003>.
41. V. Kumar, F. Durst, and S. Ray, “Modeling Moving-Boundary Problems of Solidification and Melting Adopting an Arbitrary Lagrangian-Eulerian Approach,” *Numer. Heat Transf. Part B Fundam.*, vol. 49, no. 4, pp. 299–331, Oct. 2006, doi: [10.1080/10407790500379981](https://doi.org/10.1080/10407790500379981).
42. R. Eliodoro Chiavazzo Ing Luigi Mongibello Candidato Manfredi Neri, “Numerical simulation of PCM-based storage units to be integrated into commercial hot water storage tanks,” 2018.
43. J. H. N. Ehms, R. De Césaró Oliveski, L. A. O. Rocha, C. Biserni, and M. Garai, “Fixed grid numerical models for solidification and melting of phase change materials (PCMs),” *Applied Sciences (Switzerland)*, vol. 9, no. 20, 2019, doi: [10.3390/app9204334](https://doi.org/10.3390/app9204334).
44. S. N. AL-Saadi and Z. (John) Zhai, “Modeling phase change materials embedded in building enclosure: A review,” *Renew. Sustain. Energy Rev.*, vol. 21, pp. 659–673, 2013, doi: <https://doi.org/10.1016/j.rser.2013.01.024>.
45. M. Calati, “DEVELOPMENT AND OPTIMIZATION OF POROUS STRUCTURES FOR EFFICIENT THERMAL ENERGY STORAGE USING PHASE CHANGE MATERIALS (PCMs) FOR REFRIGERATED.” pp. 1–157, 2023.
46. M. Muhieddine, E. Canot, and R. March, “Various Approaches for Solving Problems in Heat Conduction with Phase Change,” *Int. J. Finite Vol.*, p. 19, 2009.
47. Lemmon E.C, “Phase-change techniques for finite element conduction codes,” no. July. pp. 1–23, 1979.
48. K. Morgan, R. W. Lewis, and O. C. Zienkiewicz, “An improved algorithm for heat conduction problems with phase change,” *Int. J. Numer. Methods Eng.*, vol. 12, no. 7, pp. 1191–1195, Jan. 1978, doi: <https://doi.org/10.1002/nme.1620120710>.
49. V. R. Voller and C. R. Swaminathan, “ERAL SOURCE-BASED METHOD FOR SOLIDIFICATION PHASE CHANGE,” *Numer. Heat Transf. Part B Fundam.*, vol. 19, no. 2, pp. 175–189, Jan. 1991, doi: [10.1080/10407799108944962](https://doi.org/10.1080/10407799108944962).
50. M. Cross, S. Johnson, and P. Chow, “Mapping enthalpy-based solidification algorithms onto vector and parallel architectures,” *Appl. Math. Model.*, vol. 13, no. 12, pp. 702–709, 1989, doi: [10.1016/0307-904X\(89\)90163-7](https://doi.org/10.1016/0307-904X(89)90163-7).
51. E. B. S. Mettawee and G. M. R. Assassa, “Thermal conductivity enhancement in a latent heat storage system,” *Sol. Energy*, vol. 81, no. 7, pp. 839–845, 2007, doi: [10.1016/j.solener.2006.11.009](https://doi.org/10.1016/j.solener.2006.11.009).
52. K. Nakaso, H. Teshima, A. Yoshimura, S. Nogami, Y. Hamada, and J. Fukai, “Extension of heat transfer area using carbon fiber cloths in latent heat thermal energy storage tanks,” *Chem. Eng. Process. Process Intensif.*, vol. 47, no. 5, pp. 879–885, 2008, doi: <https://doi.org/10.1016/j.cep.2007.02.001>.
53. J. Fukai, M. Kanou, Y. Kodama, and O. Miyatake, “Thermal conductivity enhancement of energy storage media using carbon fibers,” *Energy Convers. Manag.*, vol. 41, no. 14, pp. 1543–1556, 2000, doi: [https://doi.org/10.1016/S0196-8904\(99\)00166-1](https://doi.org/10.1016/S0196-8904(99)00166-1).
54. F. Frusteri, V. Leonardi, S. Vasta, and G. Restuccia, “Thermal conductivity measurement of a PCM based storage system containing carbon fibers,” *Appl. Therm. Eng.*, vol. 25, no. 11, pp. 1623–1633, 2005, doi: <https://doi.org/10.1016/j.applthermaleng.2004.10.007>.
55. Y. Hamada, W. Otsu, J. Fukai, Y. Morozumi, and O. Miyatake, “Anisotropic heat transfer in composites based on high-thermal conductive carbon fibers,” *Energy*, vol. 30, no. 2, pp. 221–233, 2005, doi: <https://doi.org/10.1016/j.energy.2004.04.024>.
56. O. Sanusi, R. Warzoha, and A. S. Fleischer, “Energy storage and solidification of paraffin phase change material embedded with graphite nanofibers,” *Int. J. Heat Mass Transf.*, vol. 54, no. 19, pp. 4429–4436, 2011, doi: <https://doi.org/10.1016/j.ijheatmasstransfer.2011.04.046>.





57. P. V. S. S. Srivatsa, R. Baby, and C. Balaji, "Numerical Investigation of PCM Based Heat Sinks with Embedded Metal Foam/Crossed Plate Fins," *Numer. Heat Transf. Part A Appl.*, vol. 66, no. 10, pp. 1131–1153, Nov. 2014, doi: 10.1080/10407782.2014.894371.
58. A. Sari and A. Karaipekli, "Thermal conductivity and latent heat thermal energy storage characteristics of paraffin/expanded graphite composite as phase change material," *Appl. Therm. Eng.*, vol. 27, no. 8–9, pp. 1271–1277, 2007, doi: 10.1016/j.applthermaleng.2006.11.004.
59. J. Lopez, G. Caceres, E. Palomo Del Barrio, and W. Jomaa, "Confined melting in deformable porous media: A first attempt to explain the graphite/salt composites behaviour," *Int. J. Heat Mass Transf.*, vol. 53, no. 5, pp. 1195–1207, 2010, doi: <https://doi.org/10.1016/j.ijheatmasstransfer.2009.10.025>.
60. D. Zhou and C. Y. Zhao, "Experimental investigations on heat transfer in phase change materials (PCMs) embedded in porous materials," *Appl. Therm. Eng.*, vol. 31, no. 5, pp. 970–977, 2011, doi: <https://doi.org/10.1016/j.applthermaleng.2010.11.022>.
61. O. Mesalhy, K. Lafdi, A. Elgafy, and K. Bowman, "Numerical study for enhancing the thermal conductivity of phase change material (PCM) storage using high thermal conductivity porous matrix," *Energy Convers. Manag.*, vol. 46, no. 6, pp. 847–867, 2005, doi: <https://doi.org/10.1016/j.enconman.2004.06.010>.

